Journal of Institute of Science and Technology, 26(1), 43-50 (2021)
ISSN: 2469-9062 (print), 2467-9240 (e)
https://doi.org/10.3126/jist.v26i1.37817

Research Article

STRUCTURAL, ELECTRONIC AND MAGNETIC PROPERTIES OF DEFECTED WATER ADSORBED SINGLE LAYER MoS_2

Hari Krishna Neupane[1,2], **Narayan Prasad Adhikari**[2*]

[1]*Department of Physics, Amrit Campus, Tribhuvan University, Kathmandu, Nepal*
[2]*Central Department of Physics, Tribhuvan University, Kathmandu, Nepal*
[*]*Corresponding author: narayan.adhikari@cdp.tu.edu.np*

*(**Received**: January 19, 2021; **Revised**: May 05, 2021; **Accepted**: June 04, 2021)*

ABSTRACT

Water adsorbed in MoS_2 (w_{ad}-MoS_2), 1S atom vacancy defect in w_{ad}-MoS_2 (1S-w_{ad}-MoS_2), 2S atoms vacancy defects in w_{ad}-MoS_2 (2S-w_{ad}-MoS_2), and 1Mo atom vacancy defect in w_{ad}-MoS_2 (Mo-w_{ad}-MoS_2) materials were constructed, and their structural, electronic, and magnetic properties were studied by spin-polarized density functional theory (DFT) based first-principles calculations. The w_{ad}-MoS_2, 1S-w_{ad}-MoS_2, 2S-w_{ad}-MoS_2, and Mo-w_{ad}-MoS_2 materials were found stable. From band structure calculations, w_{ad}-MoS_2, 1S-w_{ad}-MoS_2 and 2S-w_{ad}-MoS_2 materials open energy bandgap of values 1.19 eV, 0.65 eV and 0.38 eV respectively. Also, it was found that the conductivity strength of the material increases with an increase in the concentration of S atom vacancy defects in the structure. On the other hand, the Mo-w_{ad}-MoS_2 material has metallic properties because energy bands of electrons crossed the Fermi energy level in the band structure. For the investigation of magnetic properties, the density of states (DoS) and partial density of states (PDoS) calculations were used and found that w_{ad}-MoS_2, 1S-w_{ad}-MoS_2, and 2S-w_{ad}-MoS_2 are non-magnetic materials, while Mo-w_{ad}-MoS_2 is a magnetic material. The total magnetic moment of Mo-w_{ad}-MoS_2 has a value of 2.66 μ_B/cell, due to the arrangement of unpaired up-spin and down-spin of electrons in 3s & 3p orbitals of S atoms; and 4p, 4d & 5s orbitals of Mo atoms in the material.

Keywords: DFT, Magnetic moment, Spins, Vacancy defects, Water adsorbed MoS_2.

INTRODUCTION

Molybdenum disulphide (MoS_2) is a two dimensional (2D) transition metal dichalcogenides (TMDS) material. It has a direct band gap semiconductor of band gap energy 1.80 eV (Mak *et al.,* 2010), although it was reported 1.16 eV in the bulk state using density functional theory implemented in tight binding linear Muffin-tin orbital approach (Sedhain & Kaphle, 2017). The band gap is opened between the lowest energy of the conduction band and the highest energy of the valence band at the k-point. MoS_2 has a high carrier mobility of 200 cm^2/Vs, and a high on/off current ratio of 10^8 at room temperature, so it is used in the field of FETs and photo-detectors (Radisavljevic *et al.*, 2011; Jean & Konor, 2007). Both the theoretical and experimental research groups have studied the physical properties of monolayer MoS_2.

The physical properties are very sensitive to pressure, electric field and strain, because transitions from semiconductors to metal are observed in monolayer MoS_2 due to strain and electric field (Yun *et al.,* 2012; Ataca & Ciraci, 2011; Ataca *et al.,* 2011; Johari & Shenoy, 2012; Kumar & Ahluwalia, 2012; Scalise *et al.,* 2012; Li & Chen, 2014). So, MoS_2 is used in the field of optoelectronics and nanoelectronics devices, as solid lubricants and as catalytic surfaces for hydrogen storage (Novoselov *et al.,* 2012; Neto *et al.,* 2009; Li & Zhu, 2015; Radisavljevic *et al.,* 2011). Hence, it is known as some of the most studied nano-materials due to their different array of technological and industrial applications. MoS_2 has also been studied for the adsorption of water molecules because the devices made by MoS_2 sometimes have to be used in a moisture environment. The physical properties (electronic, magnetic, and tribologic) are affected by adsorbed molecules (like water molecule, hydrogen atom) in monolayer MoS_2 (Panitz *et al.,* 1988; Zhao *et al.,* 2010; Pantha & Adhikari, 2015; Pantha *et al.,* 2020). Hence, the adsorption of a water molecule in monolayer MoS_2 is one of the promising approaches to modify and deceive unwanted properties of any constituent. The water adsorbed MoS_2 losses its lubricity because water-driven oxidation in MoS_2 material leads to the formation of molybdenum trioxide (MoO_3) (Liang *et al.,* 2008; Liang *et al.,* 2011).

Defects in the structure are one of the promising approaches to adapt and exploit the unwanted properties of materials. Hence, they influence the properties of materials in solids (Kettel *et al.,* 1996). The electronic and magnetic properties are attractive properties of the materials. Mo vacancy defect in material develops magnetic properties (Neupane & Adhikari, 2020). Magnetic materials have conceivable applications in the fields of biomedicine, molecular biology, biochemistry, diagnosis, catalysis, nanoelectronic devices, magnetic sensors, computers, magnetic recording media, electric power generators, and transformers (Makarova *et al.,* 2019; Peng *et al.,* 2016).

To our best knowledge, electronic and magnetic properties Mo vacancy defect and S vacancy defect respectively in water adsorbed MoS_2 material have not been reported. Therefore, in present work, we studied the structural, electronic, and magnetic properties of Mo vacancy defect in water adsorbed MoS_2 material, and S vacancy defects in water adsorbed MoS_2 material by spin-polarized DFT theory based first-principles calculations.

MATERIALS AND METHODS

First-principles calculation was performed to investigate the structural, electronic, and magnetic properties of water adsorbed in MoS_2, and Mo & S atoms vacancy defects in water adsorbed MoS_2 materials within the framework of DFT theory (Hohenberg & Kohn, 1964), using Quantum ESPRESSO (QE) computational package (Giannozzi *et al.,* 2009), and structure visualization program XCrySDen (Kokalj, 1999). The electronic exchange and correlation effects in the systems were treated by generalized gradient approximation (GGA) using Perdew-Burke-Ernzerhof (PBE) (Perdew *et al.,* 1996). Rappe-Rabe-Kaxiraas-Joannopoulos (RRKJ) model of ultra-soft pseudo-potentials was used to explain the chemically active valence electrons in our calculations. The Broyden-Fletcher-Goldfarb-Shanno (BFGS) algorithm (Pfrommer *et al.,* 1997) was used to relax the structures until the total energy change was less than 10^{-4} Ry between two consecutive self-consistent field (SCF) steps and each component of force acting was less than 10^{-3} Ry/Bohrs to get geometrically optimized structures. The unit cell was optimized to lattice parameter (a), kinetic energy cut-off (E_{cut}) for plane-wave and the number of k-points along 'x' and 'y' axes, respectively.

The values of lattice constant (a = 3.18 Å), kinetic energy cut-off (E_{cut} = 35 Ry), charge density cut-off (ρ = 350 Ry), and a mesh of (16×16×1) k-points of MoS_2 unit cell were obtained from the convergence test. A mesh of (16×16×1) k-points of MoS_2 unit cell was found from the plot of the total energy versus the number of k-points, where the energy of the unit cell of monolayer MoS_2 was almost constant after n_{kx} =16. Hence, in the unit cell of MoS_2, a mesh of (16×16×1) k-points was used for the Brillouin-zone integration. For the (3×3) supercell structure of MoS_2, the lattice constant was three times that of the unit cell and a mesh of k-points was reduced to (6×6×1). The reduction of the mash was due to the relation of direct and reciprocal lattice geometries. The Marzarri-Vanderbilt (MV) (Marzari *et al.,* 1999), method of smearing with a small width of 0.001Ry was used. In addition, 'david' diagonalization method was chosen with 'plain' mixing mode and a mixing factor of 0.6 for self-consistency. Spin-polarized calculations were allowed to study the magnetic properties of the systems. For band structure calculations, 100 k-points were chosen along the high symmetric points connecting the reciprocal space. For the density of states (DoS) and partial density of states (PDoS) calculations, denser meshes of (12×12×1) k-points were taken.

In the present work, water adsorbed MoS_2 structure, and Mo & S atoms vacancy defects in water adsorbed MoS_2 structures were prepared. At first, w_{ad}-MoS_2 material was constructed by adsorbing water molecules at 2.52 Å distance above the surface of MoS_2. Then, a Mo atom vacancy defect in the w_{ad}-MoS_2 structure (Mo-w_{ad}-MoS_2) was created by removing 1Mo atom in w_{ad}-MoS_2. Similarly, 1S and 2S atoms vacancy defects in w_{ad}-MoS_2 structure (i.e. 1S-w_{ad}-MoS_2 & 2S-w_{ad}-MoS_2) were constructed by removing upper-1S atom in w_{ad}-MoS_2 and 2S (upper-1S & lower-1S) atoms in w_{ad}-MoS_2 structure respectively. All these structures were then optimized and relaxed by using the BFGS scheme for further calculations. Fig. 1 represents stable and relaxed water adsorbed in MoS_2 (w_{ad}-MoS_2), Mo atom vacancy defect in water adsorbed MoS_2 (Mo-w_{ad}-MoS_2), 1S (upper-S atom) vacancy defect in water adsorbed MoS_2 (1S-w_{ad}-MoS_2), and 2S (1S-upper & 1S-lower) atoms vacancy defects in water adsorbed MoS_2 (2S-w_{ad}-MoS_2) materials.

RESULTS AND DISCUSSION

The main findings and their interpretations are presented in this section. Spin-polarized DFT calculations were carried out for the first-principles study of w_{ad}-MoS_2, Mo-w_{ad}-MoS_2, 1S-w_{ad}-MoS_2, and 2S-w_{ad}-MoS_2 materials using computational tools Quantum ESPRESSO.

Structural analysis

The (3×3) supercell structure of monolayer MoS_2 was prepared by extending optimized primitive unit cell along 'x' and 'y' directions using structural visualization tool XCrySDen. The distance between Mo and S atoms in MoS_2 was equal to 3.18 Å. This value agrees with the experimentally reported value of 3.19 Å (Kadantsev & Hawrylak, 2012). Different stacking configurations of w_{ad}-MoS_2 material were prepared by keeping water molecules at different positions on the surface of MoS_2 material. It found that the optimized and relax structure of w_{ad}-MoS_2 material formed by adsorbing water molecules at 2.52 Å distance above the top surface of MoS_2 was more stable than other configurations. This stable structure is shown in Fig. 1(a).

The stability of structures was determined by binding energy calculations. The greater value of binding energy was more favorable for the stability of the system. The binding energy of w_{ad}-MoS_2 was calculated by using the relation (Vu *et al.,* 2020), as depicted in equation (1);

$$E_b = E_{water} + E_{MoS2} - E_{water/MoS2} \quad (1)$$

Where, E_{water}, $E_{MoS2,}$ and $E_{water/MoS2}$ represent ground state energy of relaxing water molecule, monolayer MoS_2, and water adsorbed in monolayer MoS_2 materials, respectively.

After that, Mo-w_{ad}-MoS_2, 1S-w_{ad}-MoS_2, and 2S-w_{ad}-MoS_2 structures were prepared by removing 1Mo atom, upper-1S atom, and 2S (upper-1S & lower-1S) atoms, respectively, in the w_{ad}-MoS_2 structure. Where, out of 9 Mo atoms in w_{ad}-MoS_2, the concentration of Mo atom in Mo vacancy defect w_{ad}-MoS_2 structure was found to be 11.11 %. Also, the concentration of S atoms in 1S vacancy defect w_{ad}-MoS_2 and 2S vacancy defects w_{ad}-MoS_2 structures were found to be 3.04 % and 7.41 %, respectively. The defects formation energy of these materials was calculated by the relation (Hou *et al.*, 2012), as given by equation (2);

$$E_f = E_{Td} + n_d\mu_d - E_{TP} \quad (2)$$

Where E_{Td} is the total energy of a supercell with the defects, n_d is the numbers of defects atoms removed from the perfect supercell to introduce a vacancy, μ_d is chemical potential of defects atoms, E_{TP} is the total energy of the neutral perfect supercell. The calculated defect formation energy of Mo-w_{ad}-MoS_2, 1S-w_{ad}-MoS_2 and 2S-w_{ad}-MoS_2 materials have values 0.68 eV, 0.58 eV and 0.82 eV, respectively. The lower value of defect formation energy means, materials are more stable. Thus, 1S-w_{ad}-MoS_2 is more stable than 2S-w_{ad}-MoS_2 & Mo-w_{ad}-MoS_2 materials. The obtained defect formation energy values are comparable with the defect formation energy of other 2D materials (Neupane & Adhikari, 2021). The defective structures were then relaxed by using the BFGS method. The relaxed-stable Mo-w_{ad}-MoS_2, 1S-w_{ad}-MoS_2 & 2S-w_{ad}-MoS_2 materials are shown in Figs. 1(c), 1(e) & 1(g), respectively. The binding energy of these materials is given in Table 1.

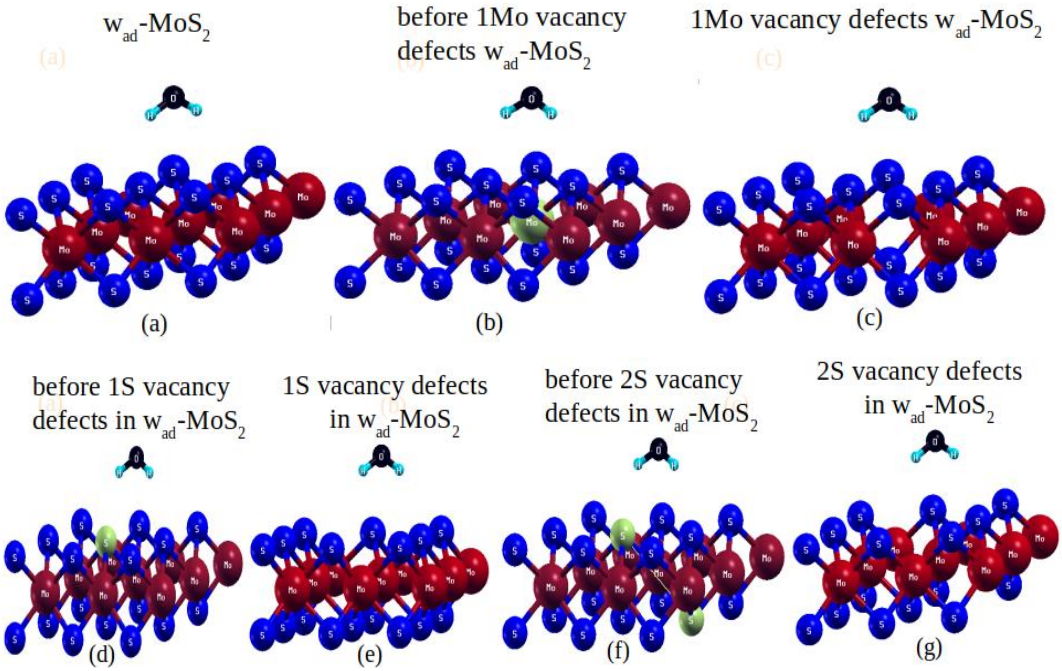

Fig. 1. (a) Water adsorbed MoS_2 structure, (b) Before 1Mo atom vacancy defect in water adsorbed MoS_2 structure, (c) 1Mo atom vacancy defect in water adsorbed MoS_2 structure, (d) Before upper-1S atom vacancy defect in water adsorbed MoS_2 structure, (e) Upper-1S atom vacancy defect in water adsorbed MoS_2 structure, (f) Before 2S atoms vacancy defects in water adsorbed MoS_2 structure (g) 2S atoms vacancy defects in water adsorbed MoS_2 structure

Electronic properties

The electronic properties of w_{ad}-MoS_2, Mo-w_{ad}-MoS_2, 1S-w_{ad}-MoS_2, and 2S-w_{ad}-MoS_2 materials were studied by the analysis of band structure calculations. To know the effect of the adsorbed water molecule in (3×3) supercell of monolayer MoS_2, first need to understand the electronic properties of (3×3) supercell structure of MoS_2. It is a wide band gap semiconductor of band gap value 1.65 eV (Neupane & Adhikari, 2020), this value is close to the experimentally reported value of 1.80 eV (Phuc *et al.*, 2018). The bandgap energy of w_{ad}-MoS_2 was found to be 1.19 eV which is less than the reported band gap energy value of supercell MoS_2.

Therefore, the band gap energy of w_{ad}-MoS_2 was reduced due to the adsorption of the water molecule in pure MoS_2 super cell structure as shown in Fig. 2(a). Similarly, we have calculated the band gap energy values of 1S-w_{ad}-MoS_2 and 2S-w_{ad}-MoS_2 materials from their band structure plots as shown in Figs. 2(b) & 2(c), respectively, wherein all band structure plots, the x-axis represents high symmetric points in the first Brillouin-zone and the y-axis represents the corresponding energy values.

The band gap energy value of these materials was found to be 0.65 eV and 0.38 eV, respectively. These values are less than the band gap energy value of w_{ad}-MoS_2. Hence, from all these calculations, we concluded that w_{ad}-MoS_2, 1S-w_{ad}-MoS_2, and 2S-w_{ad}-MoS_2 materials resemble the nature of semiconductors. But, the conductivity strength of the material increases with an increase in its defect concentration. Also, the band structure of Mo-w_{ad}-MoS_2 was analyzed, and found that the energy band of electrons crossed the Fermi energy level as shown in Fig. 2(d). Hence, Mo-w_{ad}-MoS_2 is metallic in nature.

Table 1. Fermi energy (E_f), Fermi energy shift (E_s), band gap energy (E_g), binding energy (E_b), defects formation energy (E_d), total magnetic moment (M), and magnetic moment (μ) due to up-spin and down-spin of electrons in 4p, 4d & 5s orbitals of Mo atoms; 3s & 3p orbitals of S atoms; 2s & 2p orbitals of O atom; 1s orbital of H atoms; of w_{ad}-MoS_2, 1S-w_{ad}-MoS_2, 2S-w_{ad}-MoS_2 and Mo-w_{ad}-MoS_2 materials

	w_{ad}-MoS_2	1S-w_{ad}-MoS_2	2S-w_{ad}-MoS_2	Mo-w_{ad}-MoS_2
E_f (eV)	-2.04	-2.02	-2.10	-2.48
E_s (eV)	-	0.02	0.06	0.44
E_g (eV)	1.19	0.65	0.38	-
E_b (eV)	0.15	0.13	0.10	0.08
E_d (eV)	-	0.58	0.82	0.68
μ-due to 4p of Mo atoms (μ_B/cell)	0.00	0.00	0.00	0.20
μ-due to 4d of Mo atoms (μ_B/cell)	0.00	0.00	0.00	0.66
μ-due to 5s of Mo atoms (μ_B/cell)	0.00	0.00	0.00	0.02
μ-due to 3s of S atoms (μ_B/cell)	0.00	0.00	0.00	0.04
μ-due to 3p of S atoms (μ_B/cell)	0.00	0.00	0.00	1.74
μ-due to 2s of O atom (μ_B/cell)	0.00	0.00	0.00	0.00
μ-due to 2p of O atom (μ_B/cell)	0.00	0.00	0.00	0.00
μ-due to 1s of H atoms (μ_B/cell)	0.00	0.00	0.00	0.00
Total magnetic moment M (μ_B/cell)	0.00	0.00	0.00	2.66

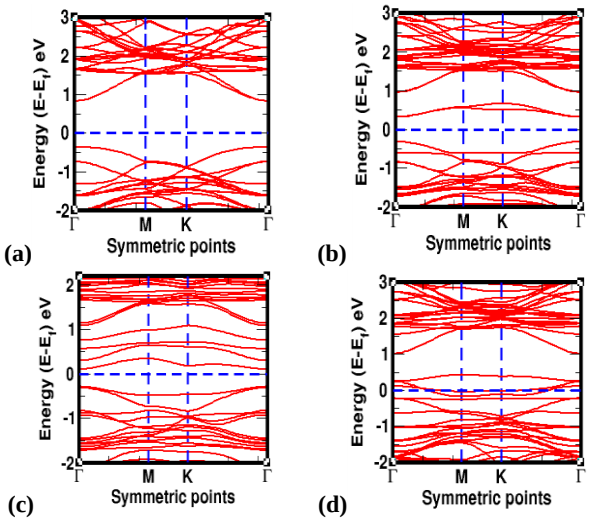

Fig. 2. (a) Band structure of (a) water adsorbed MoS_2 material, (b) upper-1S atom vacancy defect in water adsorbed MoS_2 material, (c) 2S atoms vacancy defects in water adsorbed MoS_2 material, (d) 1Mo atom vacancy defect in water adsorbed MoS_2 material

The metallic and semiconductor nature in defected materials were obtained because the edges and vacancies are very sensitive locations for molecular adsorption due to the under-coordination of atoms in the edge or around the vacancy. They also play a special role either in determining the geometrical conformation of layered materials and inducing modifications of the electronic properties of the layers themselves. It is know that electronic configurations of valence electrons in Mo, S, O and H atoms are [Kr] $4d^5$ $5s^1$, [Ne] $3s^2$ $3p^4$, [He] $2s^2$ $2p^4$ and $1s^1$, respectively. Each Mo atom has one unpaired up-spin in sub-orbital 5s and $4d_{xy}$, $4d_{xz}$, $4d_{yz}$, $4d_{x^2-y^2}$, $4d_{z^2}$; S atom has paired spins (up-spin and down-spin) in $3p_x$ sub-orbital and one unpaired up-spin in $3p_y$, $3p_z$ sub-orbital, and each O atom contains paired spins in $2p_x$ sub-orbital and single unpaired up-spin in $2p_y$ and $2p_z$ sub-orbital, H atom has single unpaired up-spin in 1s orbital. Due to the arrangement of unpaired up and down spin states of electrons in the orbitals of atoms in all w_{ad}-MoS_2, 1S-w_{ad}-MoS_2, 2S-w_{ad}-MoS_2 and Mo-w_{ad}-MoS_2 materials developed different values of Fermi energy. The Fermi energy values of w_{ad}-MoS_2, 1S-w_{ad}-MoS_2, 2S-w_{ad}-MoS_2 and Mo-w_{ad}-MoS_2 materials were found -2.04 eV, -2.02

eV, -2.10 eV and -2.48 eV, respectively. Besides, shifting of Fermi energy values of 1S-w_{ad}-MoS_2, 2S-w_{ad}-MoS_2 and Mo-w_{ad}-MoS_2 materials are 0.02 eV, 0.06 eV and 0.44 eV, respectively, which are given in Table 1. This is due to the movement of charges in the structures. Moreover, we have carried out DoS and PDoS calculations to understand the electronic and magnetic properties of materials. The DoS and PDoS plots of w_{ad}-MoS_2, 1S-w_{ad}-MoS_2, 2S-w_{ad}-MoS_2, and Mo-w_{ad}-MoS_2 materials are shown in Figs. 3(a-d) and Figs. 4(a-d), respectively, where the vertical dotted line represents Fermi energy levels of respective structures.

Magnetic properties

The magnetic moment of materials can be calculated from DoS and PDoS analysis. DoS and PDoS of up and down spin states of electrons in the orbitals of atoms in the materials were symmetrically distributed means, materials have non-magnetic properties, and asymmetrically distributed means, and materials have magnetic properties. The DoS and PDoS plots of w_{ad}-MoS_2, 1S-w_{ad}-MoS_2, 2S-w_{ad}-MoS_2, and Mo-w_{ad}-MoS_2 materials are shown in Figs. 3(a-d) and Figs. 4(a-d), respectively. We have anatomized PDoS calculations to know the contributions of the magnetic moment given by the up-spin and down-spin of electrons in the individual orbital of atoms in materials. The detailed calculations of the magnetic moment due to spin states of electrons in the orbitals of Mo, S, O, and H atoms in PDoS of w_{ad}-MoS_2, 1S-w_{ad}-MoS_2, and 2S-w_{ad}-MoS_2 materials are given in Table 1. DoS and PDoS plots of these materials are seen symmetrically distributed near the Fermi energy level as shown in Figs. 3(a-c) and Figs. 4(a-c), respectively.

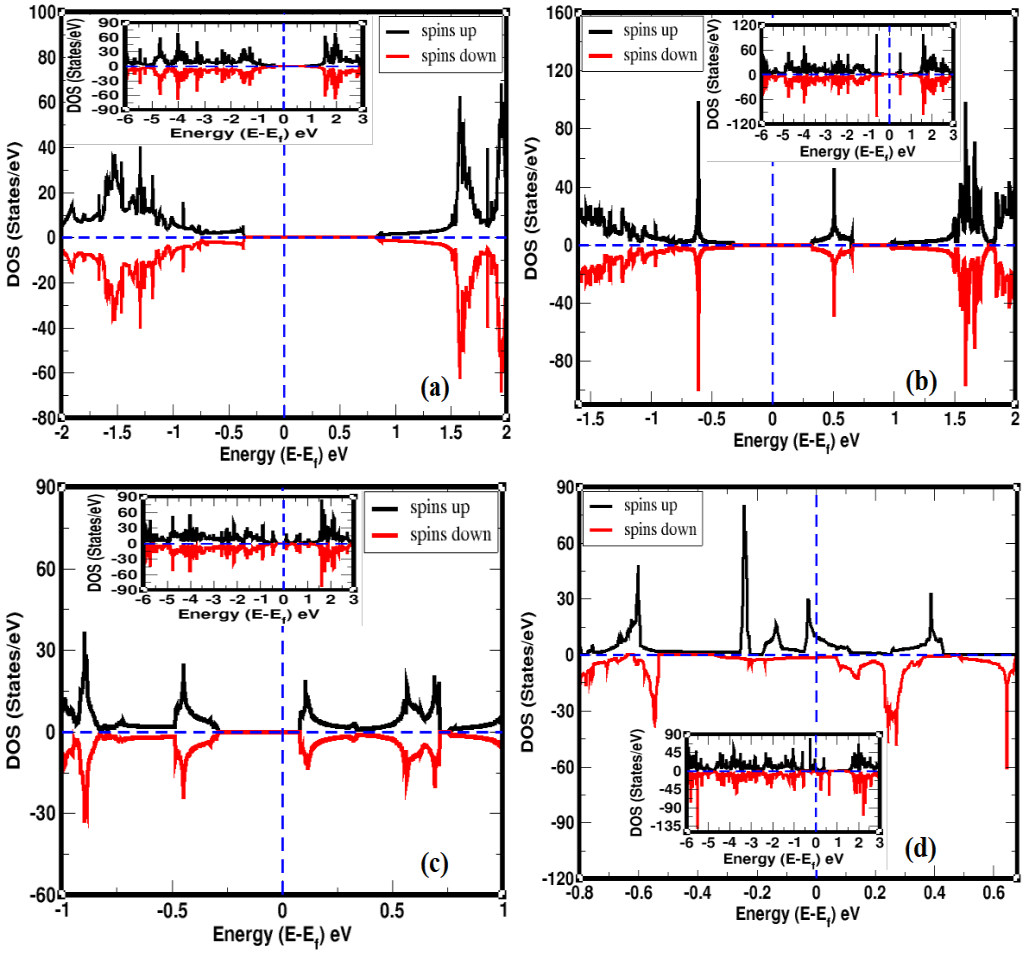

Fig. 3. (a) Total DoS of water adsorbed MoS_2 material, (b) total DoS of upper-1S atom vacancy defect in water adsorbed MoS_2 material, (c) total DoS of 2S atoms vacancy defects in water adsorbed MoS_2 material, (d) total DoS of 1Mo atom vacancy defect in water adsorbed MoS_2 material

Also, it was found that net magnetic moment given by up and down spin of electrons in 4p, 4d & 5s orbitals of Mo atoms; 3s & 3p orbitals of S atoms; 2s & 2p orbitals of O atom; and 1s orbital of H atoms have zero value. This is because; adsorbed water molecule reduces chemical activity in the lattice structures of w_{ad}-MoS_2, 1S-w_{ad}-MoS_2

and 2S-w_{ad}-MoS_2 materials. Physisorption interactions can arise when a water molecule is adsorbed in this type of structure. Therefore, w_{ad}-MoS_2, 1S-w_{ad}-MoS_2, and 2S-w_{ad}-MoS_2 materials have non-magnetic properties.

Furthermore, the DoS/PDoS calculation of Mo-w_{ad}-MoS_2 material was analyzed. The DoS and PDoS of up-spin and down-spin states of electrons near the Fermi level were asymmetrically distributed, as shown in Figs. 3(d) and 4(d). Hence, the Mo-w_{ad}-MoS_2 material has magnetic properties. Also, the contributions of the magnetic moment due to the distribution of spins of electrons in the individual orbital of atoms presented in Mo-w_{ad}-MoS_2 material are given in Table 1. The magnetic moment developed in the material due to up-spin and down-spin of electrons in 4p, 4d & 5s orbitals of Mo atoms are 0.20 μ_B/cell, 0.66 μ_B/cell & 0.02μ_B/cell; 3s & 3p orbitals of S atoms were 0.04μ_B/cell & 1.74μ_B/cell; and 2s & 2p orbitals of O atom, 1s orbital of H atoms were 0.00 μ_B/cell values, respectively. It means dominant contributions of magnetic moments are given by spins of 4p & 4d orbitals of Mo atoms and 3s & 3p orbitals of S atoms in the material. These values of the magnetic moment were calculated by subtraction between the values of the magnetic moment given by total up-spins and total down-spins of electrons in the orbitals of atoms present in Mo-w_{ad}-MoS_2 material. Hence, from these calculations, we found that the total magnetic moment of Mo-w_{ad}-MoS_2 has a value of 2.66 μ_B/cell. The positive value of magnetic moment means the up-spin electrons of atoms have a dominant role over the down-spin electrons of atoms. In Mo-w_{ad}-MoS_2 material, 3p orbital of S atoms and 4d orbital of Mo atoms have the principal role for the development of magnetic moment.

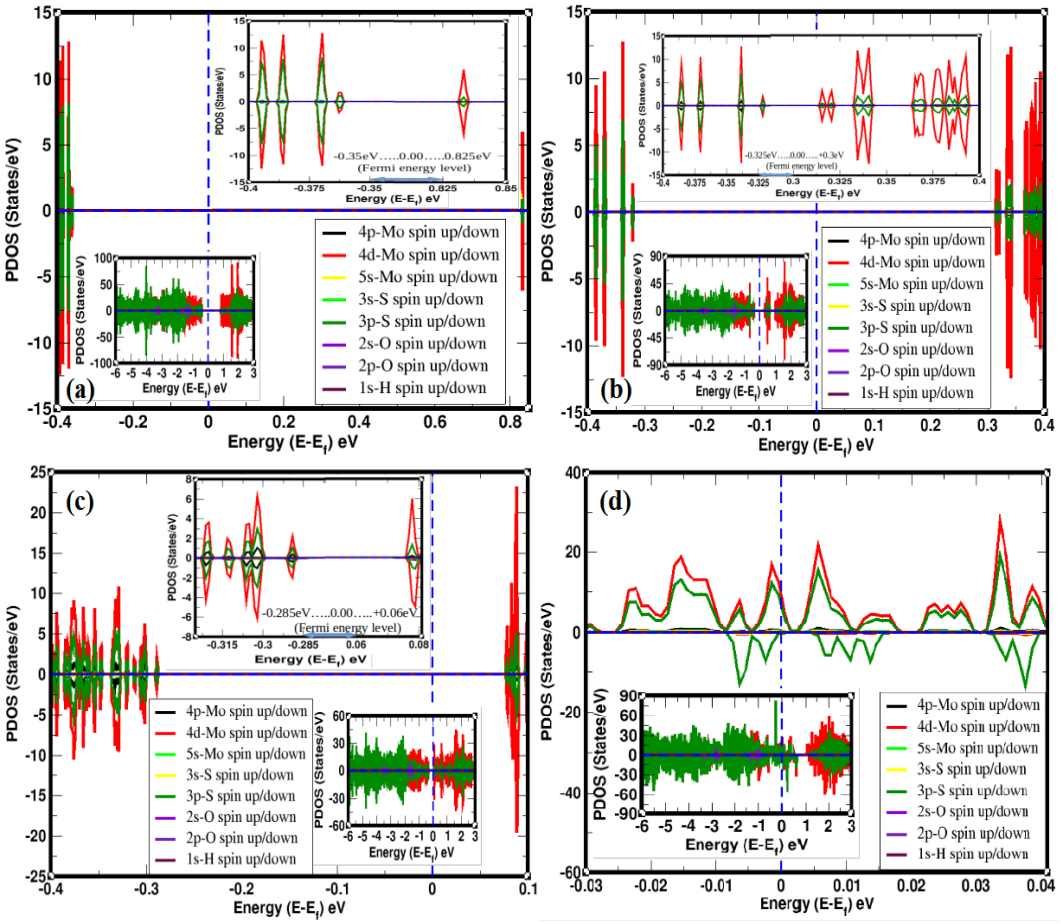

Fig. 4. PDoS of individual orbital of Mo, S, O, H atoms in (a) water adsorbed MoS_2 material, (b) upper-1S atom vacancy defect water adsorbed MoS_2 material, (c) 2S atoms vacancy defects water adsorbed MoS_2 material, and (d) 1Mo atom vacancy defect water adsorbed MoS_2 material

CONCLUSIONS

In the present work, the structural, electronic, and magnetic properties of w_{ad}-MoS_2, 1S-w_{ad}-MoS_2, 2S-w_{ad}-MoS_2, and Mo-w_{ad}-MoS_2 materials were studied by first-principles calculations based on the spin-polarized density functional theory (DFT) method. The Quantum ESPRESSO package was used for the computational work

and the XCrySDen program was used for structure visualization. By analyzing the structures, the w_{ad}-MoS_2, 1S-w_{ad}-MoS_2, 2S-w_{ad}-MoS_2, and Mo-w_{ad}-MoS_2 were found to be stable materials. From the band structure calculations, the band gap energy of w_{ad}-MoS_2, 1S-w_{ad}-MoS_2, and 2S-w_{ad}-MoS_2 materials calculated as 1.19 eV, 0.65 eV, and 0.38 eV, respectively. Therefore, these materials behave as a semiconductor. But, energy bands of electrons were crossed the Fermi energy level in the band structure of Mo-w_{ad}-MoS_2 material. Hence, Mo-w_{ad}-MoS_2 material has metallic properties. From DoS and PDoS calculations, w_{ad}-MoS_2, 1S-w_{ad}-MoS_2, and 2S-w_{ad}-MoS_2 materials are non-magnetic materials, while Mo-w_{ad}-MoS_2 is a magnetic material. Therefore, non-magnetic w_{ad}-MoS_2 changes to magnetic Mo-w_{ad}-MoS_2 material due to the presence of Mo vacancy defect. The total magnetic moment of Mo-w_{ad}-MoS_2 material has a value of 2.66 μ_B/cell. The high value of magnetic moment in Mo-w_{ad}-MoS_2 is given by distributed up-spin and down-spin in 3p orbital of S atoms and 4d orbital of Mo atoms.

ACKNOWLEDGEMENTS

HKN acknowledges the UGC Nepal for awarding the Ph. D. scholarship (PhD-75/76-S&T-09), and NPA acknowledges network project NT-14 of ICTP/OEA and UGC Nepal Grants CRG 073/74 -S&T -01.

REFERENCES

Ataca, C., & Ciraci, S. (2011). Functionalization of single-layer MoS_2 honeycomb structures. *The Journal of Physical Chemistry C*, *115*(27), 13303-13311.

Ataca, C., Sahin, H., Akturk, E., & Ciraci, S. (2011). Mechanical and electronic properties of MoS_2 nanoribbons and their defects. *The Journal of Physical Chemistry C*, *115*(10), 3934-3941.

Giannozzi, P., Baroni, S., Bonini, N., Calandra, M., Car, R., Cavazzoni, C. & Dal Corso, A. (2009). Quantum ESPRESSO: modular and open-source software project for quantum simulations of materials. *Journal of Physics: Condensed Matter*, *21*(39), 395502. https://doi.org/10.1088/0953-8984/21/39/395502

Hohenberg, P., & Kohn, W. (1964). Inhomogeneous electron gas. *Physical Review B*, *136*(3), 864. https://doi.org/10.1103/PhysRev.136.B864

Hou, Z., Wang, X., Ikeda, T., Terakura, K., Oshima, M., Kakimoto, M. A., & Miyata, S. (2012). Interplay between nitrogen dopants and native point defects in graphene. *Physical Review B*, *85*(16), 165439. https://doi.org/10.1103/PhysRevB.85.165439

Jena, D., & Konar, A. (2007). Enhancement of carrier mobility in semiconductor nanostructures by dielectric engineering. *Physical Review Letters*, *98*(13), 136805. https://doi.org/10.1103/PhysRevLett.98.136805

Johari, P., & Shenoy, V. B. (2012). Tuning the electronic properties of semiconducting transition metal dichalcogenides by applying mechanical strains. *ACS Nano*, *6*(6), 5449-5456.

Kadantsev, E. S., & Hawrylak, P. (2012). Electronic structure of a single MoS_2 monolayer. *Solid State Communications*, *152*(10), 909-913.

Kittel, C., McEuen, P., & McEuen, P. (1996). *Introduction to solid state physics* (Vol. 8, pp. 105-130). New York, USA: Wiley. ISBN: 978-81-265-3518-7

Kokalj, A., (1999). XCrySDen-a new program for displaying crystalline structures and electron densities. *Journal of Molecular Graphics and Modeling*, *17*(3-4), 176-179.

Kumar, A., & Ahluwalia, P. K. (2012). A first principle comparative study of electronic and optical properties of 1H-MoS_2 and 2H-MoS_2. *Materials Chemistry and Physics*, *135*(2-3), 755-761.

Li, X., & Zhu, H. (2015). Two-dimensional MoS_2: Properties, preparation, and applications. *Journal of Materiomics*, *1*(1), 33-44.

Li, Y., & Chen, Z. (2014). Tuning electronic properties of germanane layers by external electric field and biaxial tensile strain: a computational study. *The Journal of Physical Chemistry C*, *118*(2), 1148-1154.

Liang, T., Sawyer, W. G., Perry, S. S., Sinnott, S. B., & Phillpot, S. R. (2008). First-principles determination of static potential energy surfaces for atomic friction in MoS_2 and MoO_3. *Physical Review B*, *77*(10), 104105. https://doi.org/10.1103/PhysRevB.77.104105

Liang, T., Sawyer, W. G., Perry, S. S., Sinnott, S. B., & Phillpot, S. R. (2011). Energetics of oxidation in MoS_2 nanoparticles by density functional theory. *The Journal of Physical Chemistry C*, *115*(21), 10606-10616. https://doi.org/10.1021/jp110562n

Mak, K. F., Lee, C., Hone, J., Shan, J., & Heinz, T. F. (2010). Atomically thin MoS_2: a new direct-gap semiconductor. *Physical Review Letters*, *105*(13), 136805. https://doi.org/10.1103/PhysRevLett.105.136805

Makarova, M. V., Akaishi, Y., Ikarashi, T., Rao, K. S., Yoshimura, S., & Saito, H. (2019). Alternating magnetic force microscopy: Effect of Si doping on

the temporal performance degradation of amorphous FeCoB magnetic tips. *Journal of Magnetism and Magnetic Materials, 471*, 209-214.

Marzari, N., Vanderbilt, D., De Vita, A., & Payne, M. C. (1999). Thermal contraction and disordering of the Al (110) surface. *Physical Review Letters, 82*(16), 3296. https://doi.org/10.1103/PhysRevLett.82.3296

Neto, A. C., Guinea, F., Peres, N. M., Novoselov, K. S., & Geim, A. K. (2009). The electronic properties of graphene. *Reviews of Modern Physics, 81*(1), 109. https://doi.org/10.1103/RevModPhys.81.109

Neupane, H. K., & Adhikari, N. P. (2020). Structure, electronic and magnetic properties of 2D Graphene-Molybdenum diSulphide (G-MoS_2) Heterostructure (HS) with vacancy defects at Mo sites. *Computational Condensed Matter*, 24, e00489. https://doi.org/10.1016/j.cocom.2020.e00489

Neupane, H. K., & Adhikari, N. P. (2020). Tuning structural, electronic, and magnetic properties of C sites vacancy defects in graphene/MoS2 van der Waals heterostructure materials: A first-principles study. *Advances in Condensed Matter Physics, 2020*, 8850701. https://doi.org/10.1155/2020/8850701

Neupane, H. K., & Adhikari, N. P. (2021). First-principles study of structure, electronic, and magnetic properties of C sites vacancy defects in water adsorbed graphene/MoS_2 van der Waals heterostructures. *Journal of Molecular Modeling, 27*(3), 1-12.

Novoselov, K. S., Fal, V. I., Colombo, L., Gellert, P. R., Schwab, M. G., & Kim, K. (2012). A roadmap for graphene. *Nature, 490*(7419), 192-200.

Panitz, J. K. G., Pope, L. E., Lyons, J. E., & Staley, D. J. (1988). The tribological properties of MoS_2 coatings in a vacuum, low relative humidity, and high relative humidity environments. *Journal of Vacuum Science & Technology A: Vacuum, Surfaces, and Films, 6*(3), 1166-1170.

Pantha, N., & Adhikari, N. (2015). Structure and symmetrization of hydrogen bonding in ices VIII and X at high pressure: A density functional theory approach. *Journal of Institute of Science and Technology, 19*(2), 14-18.

Pantha, N., Thapa, S., & Adhikari, N. (2020). First-principles study of molecular adsorption of hydrogen/s on Co-adatom graphene. *Journal of Institute of Science and Technology, 25*(1), 15-23.

Peng, H. X., Qin, F., & Phan, M. H. (2016). *Ferromagnetic microwire composites: from Sensors to microwave applications*. Switzerland: Springer International Publishing. https://doi.org/10.1007/978-3-319-29276-2

Perdew, J. P., Burke, K., & Ernzerhof, M. (1996). Generalized gradient approximation made simple. *Physical Review Letters, 77*(18), 3865. https://doi.org/10.1103/PhysRevLett.77.3865

Pfrommer, B. G., Cote, M., Louie, S. G., & Cohen, M. L. (1997). Relaxation of crystals with the quasi-Newton method. *Journal of Computational Physics, 131*(1), 233-240.

Phuc, H. V., Hieu, N. N., Hoi, B. D., Phuong, L. T., & Nguyen, C. V. (2018). First principle study on the electronic properties and Schottky contact of graphene adsorbed on MoS_2 monolayer under applied out-plane strain. *Surface Science, 668*, 23-28.

Radisavljevic, B., Radenovic, A., Brivio, J., Giacometti, V., & Kis, A. (2011). Single-layer MoS_2 transistors. *Nature Nanotechnology, 6*(3), 147-150.

Scalise, E., Houssa, M., Pourtois, G., Afanas'ev, V., & Stesmans, A. (2012). Strain-induced semiconductor to metal transition in the two-dimensional honeycomb structure of MoS_2. *Nano Research, 5*(1), 43-48.

Sedhain, R., & Kaphle, G. (2017). Structural and electronic properties of transition metal dichalcogenides (MX_2) M=(Mo, W) and X=(S, Se) in bulk state: A first-principles study. *Journal of Institute of Science and Technology, 22*(1), 41-50.

Vu, T. V., Hieu, N. V., Phuc, H. V., Hieu, N. N., Bui, H. D., Idrees, M.,.. & Nguyen, C. V. (2020). Graphene/WSeTe van der Waals heterostructure: Controllable electronic properties and Schottky barrier via interlayer coupling and electric field. *Applied Surface Science, 507*, 145036. https://doi.org/10.1016/j.apsusc.2019.145036

Yun, W. S., Han, S. W., Hong, S. C., Kim, I. G., & Lee, J. D. (2012). Thickness and strain effects on electronic structures of transition metal dichalcogenides: 2H-MX_2 semiconductors (M = Mo, W; X = S, Se, Te). *Physical Review B, 85*(3), 033305. https://doi.org/10.1103/PhysRevB.85.033305

Zhao, X., & Perry, S. S. (2010). The role of water in modifying friction within MoS_2 sliding interfaces. *ACS Applied Materials & Interfaces, 2*(5), 1444-1448.